Contents list available at IJRED website
Int. Journal of Renewable Energy Development (IJRED)
Journal homepage: http://ejournal.undip.ac.id/index.php/ijred
Short Communication

Experimental Study on Solar Heat Battery using Phase Change Materials for Parabolic Dish Collectors

Ramalingam Senthil[a,*], Inbaraj Infanta Mary Priya[a], Mukund Gupta[b], Chinmaya Rath[c], Nilanshu Ghosh[d]

[a]Department of Mechanical Engineering, SRM Institute of Science and Technology, Kattankulathur, Chennai, India

[b]Department of Mechanical Engineering, University of Washington, Seattle, WA, 98195, USA

[c]Department of Electrical Sustainable Energy, Delft University of Technology, Mekelweg 4, 2628 CD Delft Netherlands

[d]Department of Sustainable Energy, KTH University, Sweden

ABSTRACT. Energy consumption has increased with the population increase, and fossil fuel dependency has risen and causing pollutions. Solar energy is suitable to provide society's thermo-electric needs. Thermal energy storage-based concentrated solar receivers are aimed at store heat energy and transportable to the applications. A cavity receiver with two-phase change materials (PCM) is experimentally investigated using a parabolic dish collector to act as the solar heat battery. The selected PCMs are $MgCl_2.6H_2O$ and KNO_3-$NaNO_3$. PCMs are chosen and placed as per the temperature zones of the receiver. The outdoor test was conducted to determine the conical receiver's storage performance using cascaded PCMs. The complete melting of PCM attains at an average receiver surface temperature of 230°C. The complete melting of the PCM in the receiver took around 30 minutes at average radiation around 700 W/m^{2,} and heat stored is approximately 5000 kJ. The estimated number of cavity receivers to be charged on a sunny day is about 10-15 according to the present design and selected PCMs, for later use.

Keywords: Solar energy, parabolic dish, thermal energy storage, heat battery, phase change material, cascaded PCM.

Article History: Received: 8th May 2021; Revised: 20th June 2021; Accepted: 26th June 2021; Available online: 30th June 2021
How to Cite This Article: Senthil, R., Priya, I.I.M., Gupta, M., Rath, C., Ghosh, N. (2021) Experimental Study on Solar Heat Battery using Phase Change Materials for Parabolic Dish Collector. *International Journal of Renewable Energy Development*, 10(4), 819-825.
https://doi.org/10.14710/ijred.2021.38376

1. Introduction

Despite using fossil fuels for our thermal needs, an alternative measure is necessary to produce sustainable energy. Solar energy is renewable and available to provide thermal and electrical power using efficient energy conversion systems. Solar radiation is available annually for about 280 days in India. Solar photovoltaic power is effectively stored in Li-ion batteries (Reddy *et al.*, 2013, Reddy *et al.*, 2015). But the major drawbacks of solar thermal systems are intermittent solar radiation and solar energy after sunshine hours. Hence, thermal energy storage (TES) plays a pivotal role in managing such radiation discontinuity. The concentrated solar collectors are helpful to attain higher temperatures for steam production and power generation, while flat plate collectors serve low to medium temperature applications (Vengadesan and Senthil, 2020a, 2020b).

The parabolic dish solar collector (PDSC) is used for medium to high-temperature applications. Solar energy application requires efficient TES to store heat during peak radiation for later uses. The phase change materials (PCM) contribute to effective thermal management because of their high energy density (Punniakodi and Senthil, 2021). The selective PCMs for PDSC are nitrates ($LiNO_3$, KNO_3, $NaNO_3$), hydrated salts, sugar alcohols, and eutectics, depending on applications (Jibin *et al.*, 2012; Reddy *et al.*, 2012).

Several researchers investigated concentrated collectors with a much focus on the poly-generation of producing heating, cooling, electricity, and green fuels (Abid *et al.*, 2020; Aghaziarati *et al.*, 2021; Yilmaz *et al.*, 2020; Ghorbani *et al.*, 2020; Shaikh *et al.*, 2021). Such systems produce high overall conversion efficiency with integrated heat storage. The collector's optical aspects, flux distribution, and mirror coatings are essential to attain the maximum output (Xiao *et al.*, 2020; Rostami *et al.*, 2021; Roosendaal *et al.*, 2020; Senthil and Nishanth, 2017). The photo-thermal efficiency improved 8% for every 0.1 increase of absorptivity.

In PDSC, the cavity-type solar receivers capture the maximum heat flux from the reflector (Bopche *et al.*, 2020; Kasaeian *et al.* 2021; López *et al.*, 2020; Santoso *et al.* 2020). A low-cost PDSC of 12.6 m^2 aperture is analyzed for heating applications (Sahu *et al.*, 2021). Cavity receivers produce more heat output than flat receivers by conserving heat flux (Yanping *et al.*, 2020). The fluid inlet temperature is significant for receiver's heat absorption

*Corresponding author: senthilr@srmist.edu.in

(Senthil *et al.* 2017a). PCM-based concentrated solar receivers enhance the overall performance by minimizing heat losses (Senthil *et al.*, 2017b, 2017c; Kalidasan *et al.*, 2020; Schöniger *et al.*, 2020; Senthil, 2020). PCM-based solar thermal systems provide promising benefits to match the thermal requirements.

The cavity receiver's smaller end is observed with a higher temperature than the larger end as per the literature. A single PCM in the solar receiver was investigated to improve the productivity of solar energy systems (Yilbasa and Khalil Anwar, 2016, Khalil Anwar *et al.*, 2016). Thus, the earlier research works are carried out with a single PCM in the solar receivers. Employment of two PCMs as per the temperature zones of a receiver is not investigated earlier. Thus, the objective of the present experimental study is to investigate the cavity receivers using cascaded PCMs to capture the varying heat flux. This current work is one of a new kind as per the authors' knowledge.

The enhancement of charging of cascaded PCMs-based solar receiver using is investigated experimentally here. A cavity receiver with two cascaded PCM is aimed to act as a solar heat battery. Outdoor tests were conducted on the PCM-cavity receiver with PDSC, and significant results are reported here. Section 1 derives the need of the study. Section 2 discusses materials and methodology. Section 3 provides a discussion on the results. Section 4 draws significant conclusions.

2. Materials and Methods

The experimental setup, experimental procedures, performance calculations, uncertainty analysis, are discussed in this section.

2.1 Experimental work

A PDSC of 16 m^2 aperture area acts as a concentrator. The detailed specifications of PDSC and conical receiver are provided in Table 1. During the actual testing, the receiver is kept at the focus of PDSC. The receiver is fixed, while the dish tracks the sun.

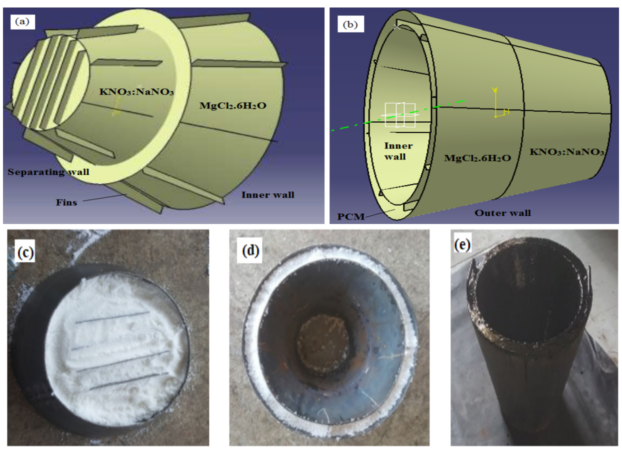

Fig. 1. The schematic layout of solar heat battery with two PCMs; (a) The inner surface with fins and separating wall for two PCMs, (b) The outer wall with annular PCM space, (c) PCM filled in the smaller end and without back cover, (d) PCM filled in the larger end without cover, (e) PCM filled and black coated cavity receiver before insulation.

There is no provision for the fluid flow through the solar heat battery as per the present design. The receiver is bifurcated with two parts to hold five kilograms of KNO_3:$NaNO_3$ at the base to capture high heat flux, and five kilograms of $MgCl_2.6H_2O$ filled near the aperture. PCMs are arranged based on the receiver's heat distribution. Fins from the receiving wall protruded to PCM to improve the heat transfer. Figure 1 shows the layout of the proposed receiver. The broader side is filled with $MgCl_2.6H_2O$ and a smaller conical annular region filled with KNO_3:$NaNO_3$. The base side PCM is filled, and the cover plate is welded. The opening side, $MgCl_2.6H_2O$, is filled, and the annular surface is welded with the proper vessel. The receiver periphery is covered with appropriate insulation. Properties of PCMs (M/s, Thermo Fisher Scientific India Pvt. Ltd, India) are given in Table 2.

2.2 *Experimental procedure*

The outdoor experiments were conducted on cavity receivers using PDSC. Figure 2 shows a schematic layout of the experimental setup. The tests were conducted in March 2018. Solar radiation, ambient, and receiver temperatures were measured. The outdoor tests started at 8.00 AM; once the receiver reached the optimum temperature of 230°C, the receiver removed from the focus and poured cold water at a temperature around 10°C to cool faster to make the receiver ready for the subsequent trial. Five tests are conducted each day at 8.00 AM, 10.00 AM, 12.00 PM, 2.00 PM, and 4.00 PM.

Table 1
The specifications of the PDSC and cavity receiver.

Item	Values
Reflector area of PDSC	16 m^2
Mirror reflectivity	0.90
Receiver major diameter	400 mm
Receiver minor diameter	350 mm
Tracking speed of PDSC	2.5 rpm
Receiver material	Mild steel
Focal distance	2700 mm
Depth of the receiver	500 mm
The wall thickness of receiver	3 mm
Geometric concentration ratio	100
Tracking	Two-axis
Seasonal tracking frequency	3-5 days
Receiver base diameter	250 mm
Fin length (PCM side)	23 mm
Fin thickness	1 mm
Width of PCM space at small end	25 mm
Mass of PCMs	5 kg each
Mass of receiver without PCM	11 kg
Receiver tilt	13°
Latitude and longitude of the site	13°N, 80°E
Insulation thickness (Glass wool)	35 mm
Reflector tracking	Two-axis
Receiver tracking	Fixed focus

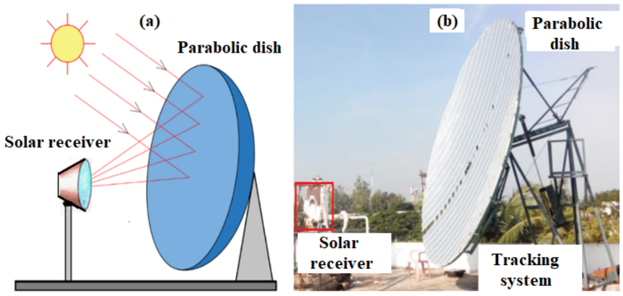

Fig. 2. PDSC and solar receiver: (a) The schematic layout, (b) Photographic view.

Table 2
Properties of selected PCMs.

Property	Values	
Chemical formula	$MgCl_2.6H_2O$	KNO_3+$NaNO_3$
Melting temperature (°C)	117	210
Density (kg/m^3)	1570	1980
Thermal conductivity (W/mK)	0.704	0.5
Enthalpy (J/g)	167	108.7
Specific heat capacity (J/gK)	2.2	1.6

An infrared thermal imaging camera (Make: Fluke Ti400) is used to measure the average receiver surface temperature during outdoor testing. The thermal imaging camera is used to measure the average surface temperature through its inbuilt function. Every minute, the temperature is observed to track the average receiver surface temperature reaching about 230°C. The experiment is stopped when attaining this temperature. This receiver temperature ensures the complete melting of both PCMs. More than 230°C also increases the total energy stored, but the PCM thermal stability is also accounted. The maximum safe working limit of PCM could be followed to avoid material loss and damage. Operating beyond a temperature of 230°C, other high-temperature PCMs can be selected. Metal PCMs are suitable for more than 500°C.

The receiver was tested for five consecutive days to monitor repeatability and reliability. The readings of the three days are illustrated in Fig. 4. The average surface receiver temperature reaches about 230°C to ensure both the PCMs melted completely in each experiment. Similar input conditions are considered for comparing the solar receivers. The outdoor testing of the cavity receiver with the cascaded PCMs repeated to ensure uniformity and repeatability. Two handles on the receiver periphery are provided to keep on the focus and transport it easily.

2.3 Performance calculations

The performance of the PDSC-solar receiver is determined based on energy stored and energy recovered. The total heat stored in PCM is given by Eq. (1),

$$Q = m_{pcm}\{(T_m - T_i) + H + C_{pcm\,(liq)}.(T_f - T_m\} \qquad (1)$$

where T_i, T_f, and T_m are the initial, final, and melting temperatures of PCM, m_{pcm} is the mass of PCM, H is the latent heat of PCM, dT is the temperature difference, C_{pcm} is the PCM specific heat.

The overall thermal efficiency is given by Eq. (2)

$$\eta_{en} = \frac{m\,C_P(T_{wf} - T_{wi})}{I_b\,A_c} \qquad (2)$$

where m is mass of water (kg), C_P is the specific heat of water (kJ/kg K), I_b is solar beam radiation (W/m^2), A_c is the PDSC aperture area (m^2), T_{wi},T_{wf} are water's initial and final temperature (K).

The storage effectiveness is defined as the ratio of actual heat stored (Q) to the maximum possible heat stored in the solar receiver.

2.4 Uncertainty analysis

An uncertainty analysis is done (Kline and McClintock, 1953; Moffat, 1988). The overall uncertainty of the experiment is determined by Eq. (3),

$$\Delta Y = \sqrt{\sum \left(\frac{\delta Y}{\delta X_i}\,\Delta X_i\right)^2} \qquad (3)$$

X is the measured quantity, Y is the overall uncertainty of the experiment (%), ΔX is uncertainty in the measured quantity (%), ΔY is uncertainty in the derived quantity (%). The uncertainty is determined based on the measurement of the mass of PCM (±0.01 kg), solar radiation using pyranometer (±5 W/m^2), temperature measurement (±0.1°C) and wind speed using anemometer (±0.1 m/s) using Eq. (4) and (5), respectively.

$$\delta\eta_{en} = \sqrt{\left(\frac{\delta\eta}{\delta\dot{m}}\right)^2(\delta\dot{m})^2 + \left(\frac{\delta\eta}{\delta I}\right)^2(\delta I)^2 + \left(\frac{\delta\eta}{\delta T_i}\right)^2(\delta T_i)^2 + \left(\frac{\delta\eta}{\delta T_o}\right)^2(\delta T_o)^2} \qquad (4)$$

$$\delta\varepsilon = \sqrt{\left(\frac{\delta\varepsilon}{\delta T_{pcm}}\right)^2(\delta T_{pcm})^2 + \left(\frac{\delta\varepsilon}{\delta T_i}\right)^2(\delta T_i)^2 + \left(\frac{\delta\varepsilon}{\delta T_o}\right)^2(\delta T_o)^2} \qquad (5)$$

The overall uncertainty of energy efficiency and storage effectiveness is determined by about ± 4.5% and 3.5%, respectively. Thus, the uncertainty is well within the acceptable range of measurements.

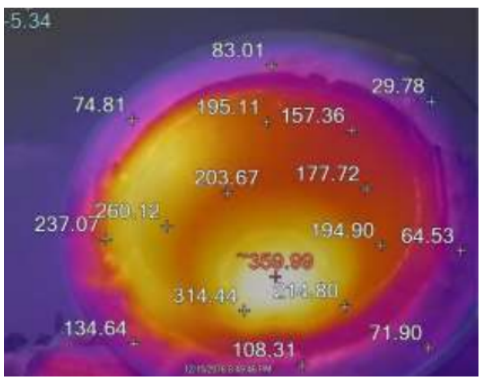

Fig. 3. The thermal image of solar receiver during the charging of PCM.

3. Results and Discussion

In this section, PCM charging, the quantity of heat stored, and the prospective applications are discussed.

3.1 PCM charging

Figure 3 shows the thermal image of temperature distribution on the cavity surface of the PCM-integrated solar receiver. The average temperature of receiver surface is determined using the in-built average function of the camera. The PCM temperature is measured using thermocouples. The heat transfer takes place from the receiver surface to PCM. The amount of heat stored is determined based on the average temperature of the PCMs.

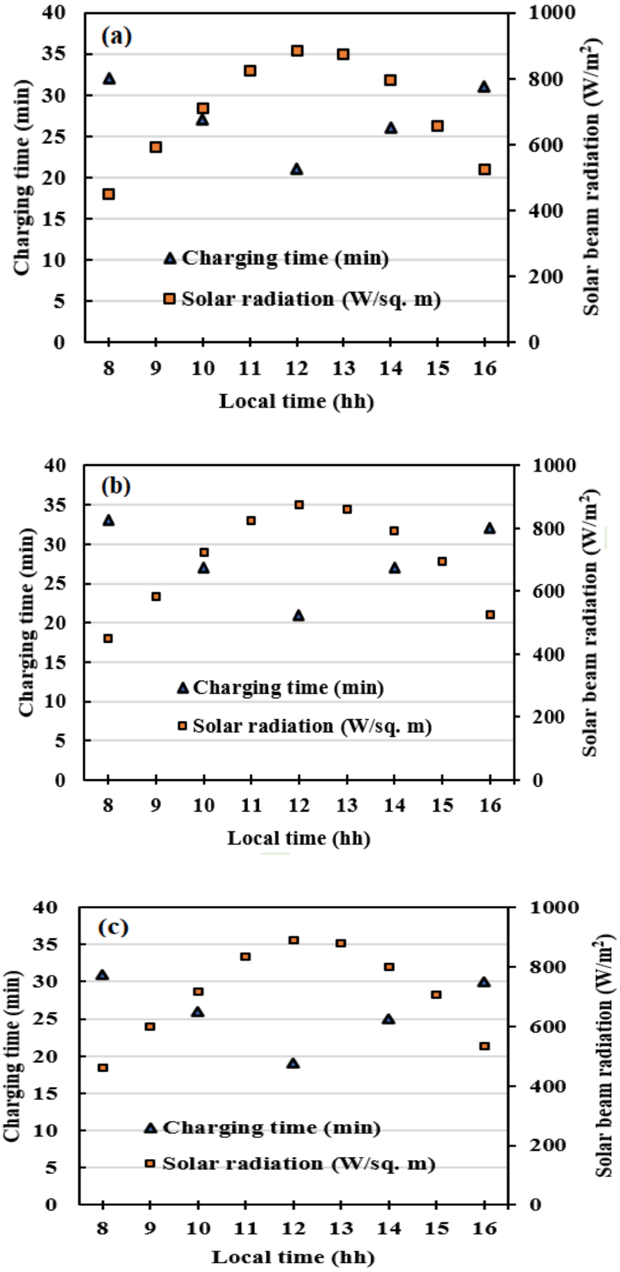

Fig. 4. (a). The charging time of receiver with PCM over the solar radiation on 21st March 2018, (b). The charging time of receiver with PCM over the solar radiation on 22nd March 2018, (c). The charging time of receiver with PCM over the solar radiation on 23rd March 2018.

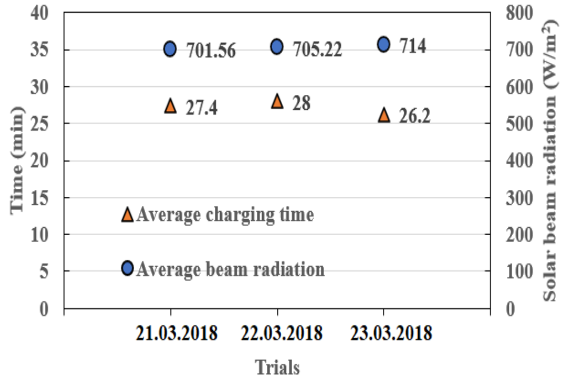

Fig. 5. The daily average charging time over the solar beam radiation during the first three days of outdoor testing (Trial 1 is on 21st March 2018; Trial 2 is on 22nd March 2018; Trial 3 is on 23rd March 2018).

Three days-testing observations are shown in Figures 4.(a)-(c). The surface temperature distribution is observed using a thermal imaging camera, and the solar radiation is measured by a weather station at the test site—higher the beam solar radiation, the charging time of PCM decreases and vice versa. The average beam solar radiation during the experimental duration over the day and the charging time of PCM is compared. The higher the radiation intensity, the charging time of PCM decreases marginally.

The conduction heat transfer dominates while melting of PCM in the both the sections of the receiver. Due to the small thickness of PCM of about 25 mm, the conduction heat transfer occurs in the PCM and the increase in temperature of PCM till the melting point and then, the melting of PCM occurs at near isothermal temperature. Natural convection in the molten PCM improves the heat transfer inside the PCM and leads to increase in temperature of PCM at the liquid state. The charging time of PCM in the solar receiver with parabolic dish collector is on par with the literature (Yilbasa and Khalil Anwar, 2016, Khalil Anwar *et al.,* 2016; Senthil, 2020; Senthil and Cheralathan, 2019).

Figure 5 shows the average beam radiation and the corresponding average time for the receiver reaching 230°C on the considered three trial days to ensure the complete PCM melting. The time is taken to melt the PCM and reach an average temperature of about 230°C is around 26-28 minutes. The slight increase or decrease in the charging time is due to average solar beam radiation during testing. The charging time of 30-35 min has been observed in the forenoon (8.00 AM) and afternoon (4.00 AM) because of low solar beam radiation. The low ambient temperature and high wind speed result in increased heat losses from the receiver with a longer charging time.

3.2 Heat stored

The heat stored in the solar heat battery is up to 5000 kJ in about 20-30 minutes at average solar radiation of around 700 W/m². Figure 6 shows the heat stored in the different components of the solar receiver in terms of sensible heat of receiver material, sensible and latent heat of PCM. Thus, from 8.00 AM to 4 PM, there is a potential of charging about several solar heat batteries with a total heat quantity of about 75,000 kJ at a concentration ratio of about 100.

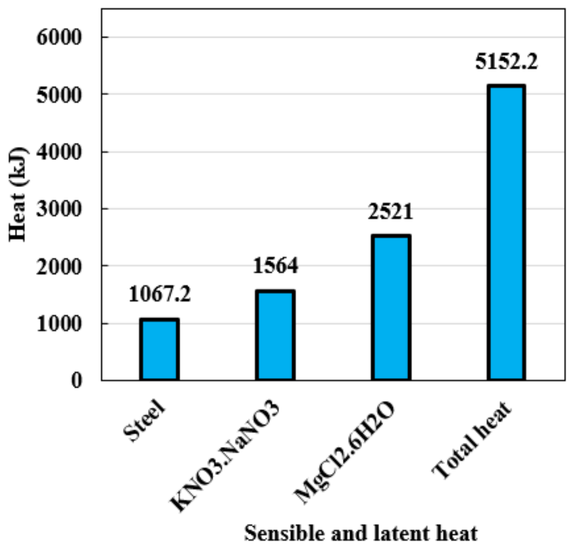

Fig. 6. The heat is stored in solar receiver material and PCM.

The heat storage effectiveness is determined based on the actual and maximum allowable temerpature of PCM in the receiver is about 0.65. The maximum allowable temperature of PCM is the critical temperature or degradation temperature of PCM. During the real-time study, the temperature is maintained at a lower than the degradation temperature to avoid the PCM mass loss. The storage effectiveness increases with the increase in PCM temerpature. Due to cascaded PCM arrangements, the operating temperatures are limited to the thermal stability of PCM. The energy efficiency of solar receiver with cascaded PCM is about 65%, based on the temperature attained by the fluid and PCM temperatures. Each heat battery can evaporate two kg of water with effective insulation of the receiver. Thus, there is a possibility of producing about 20-30 kg of steam using about 10-15 solar heat batteries using a PDSC. The heat battery must be kept inside a well-insulated container for effective later use. The thermal output of solar heat batteries using PCM is observed on par with the literature (Peiro *et al.*, 2015; Khalil Anwar *et al.*, 2016; Senthil & Cheralathan, 2019). The applications vary from domestic to industrial based on the PCM selection for the type of concentrated solar collectors.

The temperature drop of single PCM usage is faster than the multiple PCMs due to the cascaded principle. Thus, storing heat at a higher temperature is prone to heat loss to the ambient, whereas keeping the heat at two different temperatures minimizes the heat loss to the surroundings. Therefore, the use of two PCMs is helpful to capture the heat of the respective temperature zone of the solar receiver and minimize the thermal degradation to the ambient conditions.

3.3 Potential applications

Fabricated cavity receiver with PCMs is investigated to enhance receiver's heat storage. The novelty of the present design is the transportation feasibility of solar heat batteries to the application sites since the receiver mass is 21 kg. The PCM mass could be decreased or increased based on the material selection and the indented applications. Later, such receivers are taken back to the PDSC site to recharge. The selective PCM could be changed for the applications. The current selection of PCMs is suitable for hot water and cooking. For the cooking, one more vessel to be fabricated to fit into the cavity with the required provisions for personal safety. The suitable applications are hot water, cooking, space-heating, thermochemical reactions, fuel production, frying, drying, water-splitting, vapor generation, auto-clave, and medical sterilization, etc. (Ghazouani *et al.* 2019; El Mghari *et al.* 2020; Alqahtani *et al.* 2020; Touili *et al.* 2020). In addition, these heat batteries could be beneficial to hydrogen and oxygen splitting through thermochemical routes (Ghorbani *et al.* 2020; Subramaniam and Senthil, 2021). Further, the current pandemic situations, such as renewable energy-based heat batteries, could benefit the health community.

The challenges of solar heat batteries are the automated charging of PCM-receivers at the PDSC site, handling, transportation, insulation, and relevant safety measures. The PCM-receivers must be monitored and provided with the required tracking control for the safe operation against PCM's overheating during charging.

4. Conclusions

Fabrication of a cascaded receiver with PCMs is investigated to enhance the receiver's heat storage. The designed receiver stores around 5000 kJ in 30 minutes of solar concentration using PDSC at average solar radiation of about 700 W/m^2. High absorption of cavity surface coating and reflectivity of PDSC resulted from faster PCM charging. While discharging heat, a single high-temperature PCM's exergy destruction is higher than the multiple PCMs. The solar heat battery benefits domestic hot water and cooking by direct contact or with the help of highly conductive metal-based vessels. Thus, more than two PCMs may be preferable to improve the receiver's performance. The PCMs and enhancements are essential to improve commercial deployment of such solar heat batteries to meet small to large-scale energy requirements. The PCM charging is studied, but the discharging is not analyzed in the current study. Further studies are required to design a suitable heat exchange mechanism like finned vessels with thermal conductivity enhanced vessels to augment heat exchange from the cascaded PCM to practical applications.

References

Abid, M., Khan, M. S., Ratlamwala, T. A. H., & Amber, K. P. (2020). Thermo-environmental investigation of solar parabolic dish-assisted multi-generation plant using different working fluids. *International Journal of Energy Research*, 44(15), 12376-12394. https://doi.org/10.1002/er.5340.

Aghaziarati, Z., & Aghdam, A. H. (2021). Thermoeconomic analysis of a novel combined cooling, heating and power system based on solar organic rankine cycle and cascade refrigeration cycle. *Renewable Energy*, 164, 1267-1283. https://doi.org/10.1016/j.renene.2020.10.106.

Alqahtani, T., Bamasag, A., Mellouli, S., Askri, F., & Phelan, P.E. (2020). Cyclic behaviors of a novel design of a metal hydride reactor encircled by cascaded phase change materials. *International Journal of Hydrogen Energy,* 45(56), 32285-97. Https://doi.org/10.1016/j.ijhydene.2020.08.280.

Bopche, S., Rana, K., & Kumar, V. (2020). Performance improvement of a modified cavity receiver for parabolic dish concentrator at medium and high heat concentration. *Solar Energy*, 209, 57-78. https://doi.org/10.1016/j.solener.2020.08.089.

El Mghari, H., Huot, J., Tong, L., & Xiao, J. (2020). Selection of phase change materials, metal foams and geometries for improving metal hydride performance. *International Journal of Hydrogen Energy,* 45(29), 14922-39. https://doi.org/10.1016/j.ijhydene.2020.03.226.

Ghazouani, K., Skouri, S., Bouadila, S., Guizani, A.A. (2019). Thermal optimization of solar dish collector for indirect vapor generation. *International Journal of Energy Research* 43, 7240-53. https://doi.org/10.1002/er.4748.

Ghorbani, B., Mehrpooya, M., & Sadeghzadeh, M. (2020). Process development of a solar-assisted multi-production plant: Power, cooling, and hydrogen. *International Journal of Hydrogen Energy,* 45(55), 30056-30079. https://doi.org/10.1016/j.ijhydene.2020.08.018.

Jibin, A. K., Reddy, M.V., Subba Rao, G.V., Varadaraju, U.V., & Chowdari, B.V.R. (2012). Pb_3O_4 type antimony oxides MSb_2O_4 (M=Co, Ni) as anode for Li-ion batteries, *Electrochimica Acta* 71, 227-232,

Kalidasan, B., Pandey, A. K., Shahabuddin, S., Samykano, M., Thirugnanasambandam, M., & Saidur, R. (2020). Phase change materials integrated solar thermal energy systems: Global trends and current practices in experimental approaches. *Journal of Energy Storage*, 27 https://doi.org/10.1016/j.est.2019.101118

Kasaeian, A., Kouravand, A., Vaziri Rad, M. A., Maniee, S., & Pourfayaz, F. (2021). Cavity receivers in solar dish collectors: A geometric overview. *Renewable Energy*, 169, 53-79. https://doi.org/10.1016/j.renene.2020.12.106.

Khalil Anwar, M., Yilbas, B. S., & Shuja, S. Z. (2016). A thermal battery mimicking a concentrated volumetric solar receiver, *Applied Energy*, 175, 16–30.

Kline, S. & McClintock, F. (1953). Describing Uncertainties in Single-Sample Experiments. *Mechanical Engineering,* 75, 3–8.

López, O., Baños, A., & Arenas, A. (2020). On the thermal performance of flat and cavity receivers for a parabolic dish concentrator and low/medium temperatures. *Solar Energy*, 199, 911-923. https://doi.org/10.1016/j.solener.2019.07.056.

Moffat, R. J. (1988). Describing the Uncertainties in Experimental Results. *Experimental Thermal and Fluid Science* 1, 3–17.

Peiro, G., Gasia, J., Mir, L., & Cabeza, L.F. (2015). Experimental evaluation at pilot plant scale of multiple PCM (cascaded) vs. single PCM configuration for thermal energy storage, *Renewable Energy,* 83,729–736,

Punniakodi, B. M. S., & Senthil, R. (2021). A review on container geometry and orientations of phase change materials for solar thermal systems. *Journal of Energy Storage*, 36, 102452.

Reddy, M. V., Subba Rao, G. V., & Chowdari, B. V. R. (2013). Metal Oxides and Oxysalts as Anode Materials for Li Ion Batteries, *Chemical Reviews*, 113 (7), 5364-5457.

Reddy, M. V., Tse, L. Y., Bruce, W. K. Z., & Chowdari, B.V.R. (2015). Low temperature molten salt preparation of nano-SnO_2 as anode for lithium-ion batteries, *Materials Letters* 138, 231-234.

Reddy, M. V., Valerie Teoh, X. W., Nguyen, T. B., Michelle Lim, Y. Y., & B. V. R. Chowdari, (2012). Effect of 0.5 M $NaNO_3$: 0.5 M KNO_3 and 0.88 M $LiNO_3$:0.12 M LiCl Molten Salts, and Heat Treatment on Electrochemical Properties of TiO_2, *Journal of The Electrochemical Society*, 159 (6), A762.

Roosendaal, C., Swanepoel, J. K., & Le Roux, W. G. (2020). Performance analysis of a novel solar concentrator using lunar flux mapping techniques. *Solar Energy*, 206, 200-215.

Rostami, M., Pirvaram, A., Talebzadeh, N., & O'Brien, P. G. (2021). Numerical evaluation of one-dimensional transparent photonic crystal heat mirror coatings for parabolic dish concentrator receivers. *Renewable Energy*, 171, 1202-1212.

Sahu, S. K., Arjun Singh, K., & Natarajan, S. K. (2021). Design and development of a low-cost solar parabolic dish concentrator system with manual dual-axis tracking. *International Journal of Energy Research*, 45(4), 6446-6456.

Santoso, D. I., Antoko, B., & Ichsani, D. (2020). Optimizing solar dish performance using analytical flux distribution in focal region. *International Journal of Renewable Energy Development*, 9(1), 63-67.

Schöniger, F., Thonig, R., Resch, G., & Lilliestam, J. (2021). Making the sun shine at night: Comparing the cost of dispatchable concentrating solar power and photovoltaics with storage. *Energy Sources, Part B: Economics, Planning and Policy,* 16(1), 55-74.

Senthil, R. (2020). Effect of charging of phase change material in vertical and horizontal rectangular enclosures in a concentrated solar receiver. *Case Studies in Thermal Engineering*, 21. https://doi.org/10.1016/j.csite.2020.100653.

Senthil, R., & Cheralathan, M. (2019). Enhancement of the thermal energy storage capacity of a parabolic dish concentrated solar receiver using phase change materials. *Journal of Energy Storage*, 25, 100841.

Senthil, R., & Nishanth, A. P. (2017). Optical and thermal performance analysis of solar parabolic concentrator. *International Journal of Mechanical and Production Engineering Research and Development*, 7(5), 367-374.

Senthil, R., Prabhu, S., and Cheralathan, M. (2017a). Effect of heat transfer fluid input parameters on thermal output of parabolic dish solar receiver using design of experiment techniques. *International Journal of Mechanical Engineering and Technology*, 8(8), 1148-1156.

Senthil, R., Senguttuvan, P., and Thyagarajan, K. (2017b). Experimental study on a cascaded pcm storage receiver for parabolic dish collector. *International Journal of Mechanical Engineering and Technology*, 8(11), 910-917.

Senthil, R., Thyagarajan, K., and Senguttuvan, P. (2017c). Experimental study of a parabolic dish concentrated cylindrical cavity receiver with PCM. *International Journal of Mechanical Engineering and Technology,* 8(11), 850-856.

Shaikh, P. H., Lashari, A. A., Leghari, Z. H., & Memon, Z. A. (2021). Techno-enviro-economic assessment of a stand-alone parabolic solar dish stirling system for electricity generation. *International Journal of Energy Research*, https://doi.org/10.1002/er.6513.

Subramaniam, S. B., & Senthil, R. (2021). Heat transfer enhancement of concentrated solar absorber using hollow cylindrical fins filled with phase change material, *International Journal of Hydrogen Energy*, 46, 22344-22355.

Touili, S., Alami Merrouni, A., El Hassouani, Y., Amrani, A-I., & Rachidi, S. (2020). Analysis of the yield and production cost of large-scale electrolytic hydrogen from different solar technologies and under several Moroccan climate zones. *International Journal of Hydrogen Energy,* 45(51), 26785-99.

Vengadesan, E., & Senthil, R. (2020a). A review on recent development of thermal performance enhancement methods of flat plate solar water heater. *Solar Energy*, 206, 935-961.

Vengadesan, E., & Senthil, R. (2020b). A review on recent developments in thermal performance enhancement methods of flat plate solar air collector. *Renewable and Sustainable Energy Reviews*, 134, 110315.

Xiao, L., Guo, F. -., Wu, S. -., & Chen, Z. -. (2020). A comprehensive simulation on optical and thermal performance of a cylindrical cavity receiver in a parabolic dish collector system. *Renewable Energy*, 145, 878-892.

Yanping, Z., Yuxuan, C., Chongzhe, Z., Hu, X., Falcoz, Q., Neveu, P., Cheng, P., & Xiaohong, H. (2021). Experimental investigation on heat-transfer characteristics of a cylindrical cavity receiver with pressurized air in helical pipe. *Renewable Energy*, 163, 320-330.

Yilbasa, B. S., & Khalil Anwar, M. (2016). Design of a mobile thermal battery and analysis of thermal characteristics, *Journal of Renewable and Sustainable Energy*, 8(2), 024102.

Yilmaz, F., Ozturk, M., & Selbas, R. (2020). Thermodynamic investigation of a concentrating solar collector based combined plant for poly-generation. *International Journal of Hydrogen Energy,* 45(49), 26138-26155.